magnitude smaller than the uncertainties given in Table I and is, therefore, not significant.

ACKNOWLEDGMENTS

The author wishes to thank Dr. R. F. Pearson for providing the samples and Dr. T. Riste for suggesting this problem. The helpful discussions with E. Frikkee and E. J. Samuelsen are acknowledged warmly. The aid with the experimental setup given by the technical staff of our laboratory and the assistance of R. Obbes for performing the chemical analysis of the samples is gratefully appreciated.

PHYSICAL REVIEW VOLUME 178, NUMBER 2 10 FEBRUARY 1969

Theory of Magnetic Ordering in the Heavy Rare Earths*

W. E. EVENSON† AND S. H. LIU
Institute for Atomic Research and Department of Physics, Iowa State University, Ames, Iowa 50010
(Received 12 September 1968)

A detailed account is given of the calculation of the generalized susceptibility functions of Gd, Dy, Er, and Lu using realistic energy bands. These susceptibilities clearly show the influence of the Fermi-surface geometry in determining the helical ordering arrangements of the heavy rare earths, and the ferromagnetic ordering of Gd. A microscopic discussion of the magneto-elastic effect for a general ordered spin state is also presented. The first-order transition from the helical state to the ferromagnetic or conical ferromagnetic state in Tb, Dy, Ho, and Er is explained by this effect. Dy is used as an example of the application of the formalism, and a fundamental understanding is obtained of the transition between the helical and the ferromagnetic state and of the anomalous thermal expansion in both ordered states.

A MICROSCOPIC theory of the magnetic ordering of heavy rare earths must answer the following questions: (1) Why does the indirect exchange interaction support a ferromagnetic ordering in Gd but a periodic moment arrangement in other members of the group; and (2) What is the interaction that stabilizes the ferromagnetic state in Tb and Dy and the conical ferromagnetic state in Er and Ho at low enough temperatures? In an earlier publication[1] we showed, by calculating the generalized susceptibility functions of Gd, Dy, Er, and Lu, that the type of initial magnetic ordering depends sensitively on the Fermi-surface geometry as suggested by Loucks.[2] The first part of this paper is a detailed account and some extension of this work. The second part of this paper gives a general proof of the current idea that the magneto-elastic effect is the driving force which stabilizes the ferromagnetic state at low temperatures. We work out a microscopic formalism of the magnetoelastic effect for a general ordered spin state. Using Dy as an example, we obtain a fundamental understanding of the transition between the helical and the ferromagnetic states and the anomalous thermal expansion of this material in both types of ordered states.

I. THE EXCHANGE INTERACTION

A. Introduction

The magnetic ordering in the heavy rare-earth metals comes about through an indirect-exchange interaction mediated by the conduction electrons. We know that this mechanism must be the dominant one because of the insignificance of the overlap between ions in these materials. The theory for this type of exchange interaction has been worked out formally with various approximations,[3] and is known as the Ruderman-Kittel-Kasuya-Yosida (RKKY) interaction. The interaction can easily be related to a $\mathbf{q}$-dependent susceptibility $\chi(\mathbf{q})$, which is the linear response of the conduction electron system to the effective field of the ionic moments. For one atom per unit cell this susceptibility has the form[4]

$$\chi(\mathbf{q})=\frac{1}{N}\sum_{\mathbf{k},n,n'}\frac{f_{\mathbf{k}n}(1-f_{\mathbf{k}+\mathbf{q}+\mathbf{K}_0n'})}{E_{n'}(\mathbf{k}+\mathbf{q}+\mathbf{K}_0)-E_n(\mathbf{k})}, \quad (1.1)$$

where the $f_{\mathbf{k}n}$ are Fermi-Dirac distribution functions for reduced wave vector $\mathbf{k}$ and band n, the $E_n(\mathbf{k})$ are the energy bands, $\mathbf{K}_0$ is the reciprocal lattice vector necessary to reduce $\mathbf{k}+\mathbf{q}$, and we have assumed the matrix elements to be constant and have factored them out. We have dropped other constant factors for convenience. This gives $\chi(\mathbf{q})$ the dimensions of (energy)$^{-1}$.

* Work was performed in the Ames Laboratory of the U. S. Atomic Energy Commission. Contribution No. 2366.
† Danforth Foundation Fellow. Present address: Department of Physics, University of Pennsylvania, Philadelphia, Pa.
[1] W. E. Evenson and S. H. Liu, Phys. Rev. Letters **21**, 432 (1968).
[2] S. C. Keeton and T. L. Loucks, Phys. Rev. **168**, 672 (1968), and references cited therein.
[3] See the review article by T. Kasuya, in *Magnetism*, edited by G. T. Rado and H. Suhl (Academic Press Inc., New York, 1966), Vol. IIB, pp. 215–294.
[4] Reference 3, Sec. III.

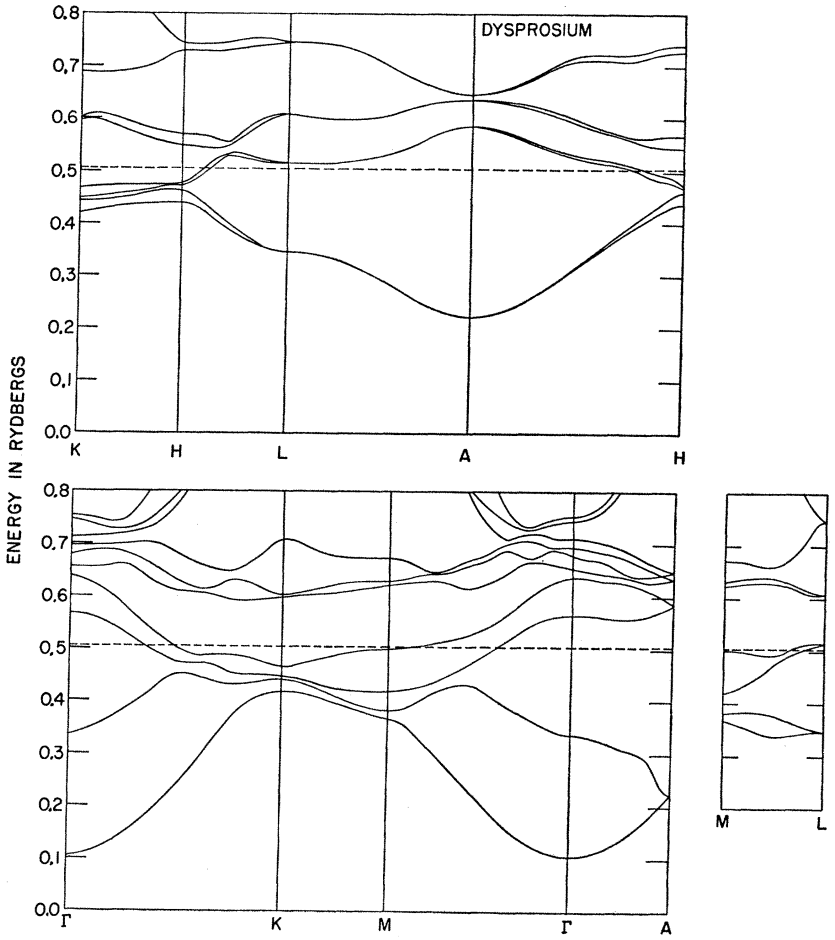

FIG. 1. Energy bands for Dy 2 along the symmetry axes of the Brillouin zone. The dashed line indicates the Fermi energy.

The stable magnetic structure will be determined by the minimum in the free energy. When the exchange term is the dominant contribution to the free energy, so that all other contributions can be neglected by comparison, then the energy of a magnetic structure characterized by wave vector $\mathbf{q}$ can be shown to be proportional to $-\chi(\mathbf{q})$.[4,5] Therefore, under these circumstances, the stable magnetic configuration will be determined by the maximum in the susceptibility $\chi(\mathbf{q})$.

The previous evaluations of $\chi(\mathbf{q})$ have been done with free-electron energy bands. The band calculations on rare-earth metals[2] have shown that they are not free-electron-like but resemble more closely the transition-element bands. The bands for Dy calculated by Keeton and Loucks[2] (the Dy2 of Ref. 2) are shown in Fig. 1, for example. The Fermi surfaces also are quite different from free-electron Fermi surfaces. We have felt that the use of free-electron bands has been the weakest point in previous calculations. Therefore, we have kept all the usual approximations[3] in the calculation of the exchange energy except that we have put realistic energy bands into Eq. (1.1) in place of the usual free-electron bands. Relativistic augmented-plane-wave energy bands for Gd, Dy, Er, and Lu were available to us from work of Keeton and Loucks.[2] These are paramagnetic bands, so our conclusions apply to the initial ordering of the metals, before the bands are too greatly perturbed by the magnetic interactions. Our results, which we have briefly discussed in a previous publication,[1] confirm the idea that the Fermi-surface geometry is the dominant factor in the determination of the maxima in the susceptibilities $\chi(\mathbf{q})$, and hence the minimum in the exchange contribution to the free energy.[2]

We are interested mainly in $\mathbf{q}$ along the line Γ to A of the Brillouin zone because all the magnetic structures observed in the heavy rare earths can be described by a wave vector in that direction.[6] Since the heavy rare earths in which we are interested all have hcp crystal structures, we can treat $\chi(q)$ in the double zone representation for $\mathbf{q}$ along the line Γ to A, q being the magnitude of a wave vector $\mathbf{q}$. We have used the energy bands in the double-zone representation so that Eq. (1.1) is the correct formulation of the suscepti-

[5] J. Villain, J. Phys. Chem. Solids 11, 303 (1959).

[6] W. C. Koehler, J. Appl. Phys. 36, 1078 (1965).

bility. This is a very good approximation because the maximum splittings on the AHL zone face due to relativistic effects were within the numerical accuracy of the bands. The relativistic form of the bands was important to the present results, however, because the relative positions of the bands and the Fermi surface were significantly modified by relativistic effects.[2,7]

Roth *et al.*[8] have discussed in some detail the relation between the geometry of the Fermi surface and the features of the susceptibility, $\chi(q)$. They show that the occurrence of nearly parallel pieces of Fermi surface such that sizable areas can be "nested" into each other by the same wave vector Q gives a logarithmic divergence in the susceptibility at the nesting Q. The nesting of points or of lines of Fermi surface gives other characteristic anomalies in the susceptibility without producing a maximum in $\chi(q)$ at any point related to the nesting Q. Lomer[9] first pointed out that nesting areas of Fermi surface are responsible for the magnetic ordering in chromium. For the rare earths, Keeton and Loucks[2] pointed out a number of places on the Fermi surface where near nesting could occur. Our calculation[1] of $\chi(q)$ gave support to their prediction.

A word should be said about the exchange matrix elements that were factored out of Eq. (1.1) as constants. Strictly speaking, they are of the form $I_{nn'}{}^2(\mathbf{k}, \mathbf{k}+\mathbf{q}+\mathbf{K}_0)$. An intermediate approximation is to call the matrix elements functions of q and n, n' only. This approximation should certainly be an improvement over constant matrix elements. In general we would expect the matrix elements to be decreasing functions of q because as q increases there should be more oscillations in the electron polarization within the ionic $4f$ shells, giving more cancellation to the overlap integral. We will discuss a possible simple approximation to $I_{nn'}{}^2(q)$ in connection with the results of the susceptibility calculation. We will see that a very simple $I^2(q)$ which decreases with q can give nice qualitative agreement with experimental magnon spectra for the rare earths.

B. Numerical Considerations

In the actual calculation of $\chi(q)$ from Eq. (1.1), we have to consider a number of numerical problems. We have neglected the temperature dependence of the Fermi functions in Eq. (1.1); the error introduced by this is only of the order of $(kT/E_F)^2$. The rest of the equation, then, is an integral over k with two sums over bands on the energy denominator, the Fermi functions being "on" or "off" switches.

We first look at the summations over the energy bands. We have calculated the susceptibility from Eq. (1.1) by treating the sums on bands in three different ways to check their convergence. Using the bands for Dy shown in Fig. 1, we calculated $\chi(q)$ three ways: once with the bands shown in the figure, once with four free-electron bands added on top of those shown, and once with only the two bands which determine the Fermi surface. There was only an essentially q-independent shift in $\chi(q)$ between these three cases. Reference to Fig. 1 shows that the bands near the Fermi energy are quite flat which would give only a q-independent contribution to $\chi(q)$ as long as they do not cut the Fermi surface to bring in the $f_k(1-f_{k'})$ factor. Those bands which are much higher or lower than the Fermi energy contribute large energy denominators to Eq. (1.1), and their contributions to the susceptibility are not effective to bring about a q dependence. All further discussion and results then will deal only with the two bands that determine the Fermi surface. This also demonstrates that the Fermi surface is crucial in the determination of the shape of the susceptibility, $\chi(q)$.

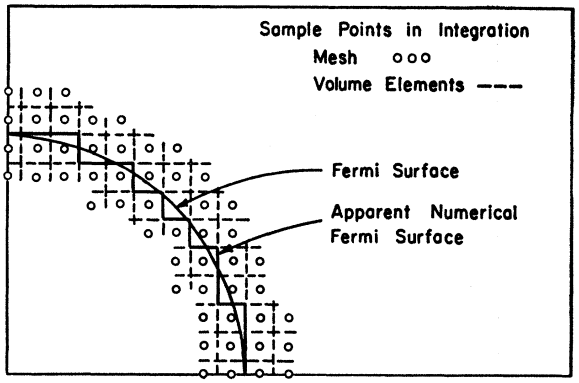

FIG. 2. Example of distortion of the Fermi surface in the numerical calculation due to the finite mesh size.

Having eliminated the band summation, we turn our attention to the $\mathbf{k}$ integration. We have used the three-dimensional extension of the trapezoidal rule to perform the integration over $\mathbf{k}$ on a mesh of 27 216 points in the Brillouin zone. The position of the finite mesh with respect to the Fermi surface may introduce some spurious peaks in the susceptibility. This is the principal source of noise in our calculation. Figure 2 shows an example of how this happens. A cross section of the Brillouin zone with a spherical Fermi surface at its center is shown. In the numerical integration, however, each mesh point is taken to be representative of the volume element in which it is centered, so the whole volume element is counted as being in or out of the Fermi surface depending on whether its mesh point is in or out. Therefore, the Fermi surface really looks to the computer like the set of shelves shown in Fig. 2, and there is nesting of areas, giving rise to spurious peaks in χ. A comparison of the results using several meshes shows that the spurious peaks move around as the mesh is changed, allowing us to eliminate them.

[7] S. C. Keeton, Ph.D. thesis, Iowa State University, Ames, Iowa, 1966 (unpublished).
[8] L. M. Roth, H. J. Zeiger, and T. A. Kaplan, Phys. Rev. **149**, 519 (1966).
[9] W. M. Lomer, Proc. Phys. Soc. (London) **80**, 489 (1962).

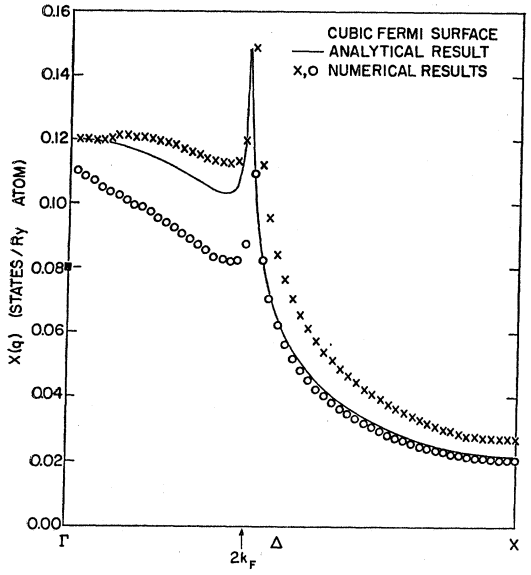

FIG. 3. Generalized susceptibility for linear bands and cubic Fermi surface.

Comparison with Fermi-surface geometry also allows us to eliminate peaks due only to the numerical procedures.

We have used two special sets of bands to develop and check the numerical procedures: (1) free-electron bands, $E(k)=\alpha k^2$ for a spherical Fermi surface, and (2) linear bands, $E(k)=|k_i|$, where k_i is the largest component of the vector $\mathbf{k}$ in absolute magnitude, for a cubic Fermi surface. The cubic Fermi surface exhibits nesting of opposite faces of the cube into each other at $Q=2k_F$. The numerical result for two different meshes is shown in Fig. 3 along with the analytical result for $\chi(q)$ in this special case. The agreement between the analytical and numerical calculations for the cubic Fermi surface is quite satisfactory, and we see that the numerical calculation gives the position and shape of the logarithmic divergence quite well. The spherical Fermi surface, on the other hand, is the worst case for spurious peaks of the type discussed above. Figure 4 shows the analytical result for the spherical Fermi surface along with the numerical $\chi(q)$ for two different meshes. Comparison of the two numerical results shows immediately that three of the peaks are spurious. We could calculate $\chi(q)$ on still a third mesh and eliminate the last peak in this way. However, it is simpler, knowing the importance of the Fermi surface to the shape of $\chi(q)$, to notice that there are no nesting areas of Fermi surface so there should be no peak in $\chi(q)$ at all. When we eliminate these peaks, we see that the numerical results agree quite satisfactorily with the analytical result.

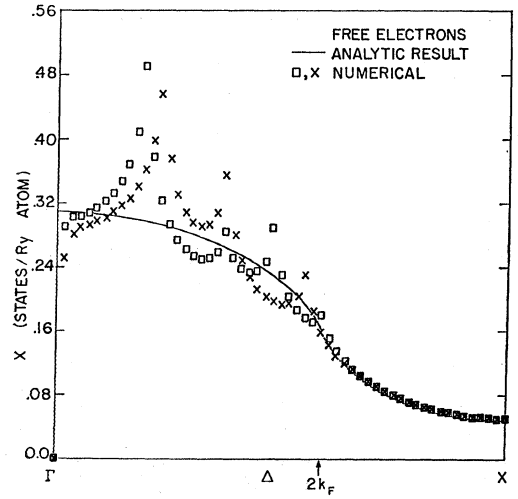

FIG. 4. Generalized susceptibility for three-dimensional free electrons.

The type of distortion of the Fermi surface introduced by the numerical integration as illustrated in Fig. 2 will not be as bad for a more complicated Fermi surface as it is for the sphere. However, one should expect considerable noise in the calculated $\chi(q)$ for this reason. We have averaged over two different meshes to reduce the noise somewhat, but a very fine mesh is needed to get a really smooth curve for $\chi(q)$.

Because of the discrete mesh we must use to perform the principal-value integral over $\mathbf{k}$, the numerical procedure cannot calculate $\chi(q)$ properly for $q=0$. When $q=0$, the denominator in Eq. (1.1) goes to zero, but the numerator also goes to zero and $\chi(0)$ has a finite value. When there is a single sheet of Fermi surface in the double zone and $\chi(q)$ is calculated with only the Fermi surface band, as in this work, it is easy to show that $\chi(0)=\frac{1}{2}N(E_F)$, where $N(E_F)$ is the density of electronic states of both spins at the Fermi energy. It is quite possible that the numerical calculation may also be poor for small, nonzero q. Special care had to be taken at small q in the case of the cubic Fermi surface to put in terms analytically for which $E(\mathbf{k}+\mathbf{q})$ and $E(\mathbf{k})$ were both equal to E_F, i.e., terms on the sides of the cube. In a more complicated Fermi surface these terms are less important than in the case of a simple cube. A comparison of the apparent limit of $\chi(q)$ as q goes to zero and $\frac{1}{2}N(E_F)$ will give an indication of how good the numerical calculation of $\chi(q)$ is for small but nonzero q. We see in Table I that our calculated

TABLE I. $\chi(q\to 0)$ compared to $\frac{1}{2}N(E_F)$.[a]

Metal	$\chi(q\to 0)$ (states/Ry/atom)	$\frac{1}{2}N(E_F)$ (states/Ry/atom)
Gd	16	14.25
Dy1	13.5	13.85
Dy2	14	12.15
Er1	11.5	12.15
Er2	12	11.8
Lu	12	12.75

[a] Reference 4.

$\chi(q\rightarrow 0)$ is within the 10–20% uncertainty in $\frac{1}{2}N(E_F)$ for the heavy rare earths, indicating that the numerical calculation is reasonably good except for $q=0$ in these cases.

The uncertainties in the energy bands which were used to calculate $\chi(q)$ led us to investigate the effects of shifting the Fermi energy up or down from the value calculated by Keeton and Loucks. As we point out below, the results are changed only by a remarkably small amount with these variations in Fermi energy. We have written a program which maps out the Fermi surface and plots appropriate cross sections to enable us to watch the changes in Fermi surface along with changes in $\chi(q)$ for various Fermi energies.

C. Results

We have shown the calculated susceptibilities along with Fermi surface cross sections for Gd, Dy, Er, and Lu in a previous publication.[1] Table II shows a comparison between the magnetic Q as determined from experiment and as determined from the beginning of the maximum in $\chi(q)$ both for the calculated Fermi energy and for a Fermi energy 0.005 Ry higher than the calculated one. (Dy1, Dy2 and Er1, Er2 correspond to different potentials used in the band calculations for Dy and Er as noted in Ref. 2.) The agreement with experiment seems to be quite satisfactory. The slightly better agreement for the higher Fermi energy is not significant because of the uncertainties in the input bands themselves. What does seem to be significant, however, is the stability of the results with respect to variations of the Fermi energy. We have considered the effect of varying the Fermi energy up or down by 0.005 Ry for all six sets of energy bands that we used: Gd, Dy1, Dy2, Er1, Er2, and Lu. The Fermi surfaces and the susceptibility curves change gradually in all cases.

Keeton and Loucks[2] pointed out that the existence of the "webbing" in the Fermi surfaces of Dy, Er, and Lu was probably important in establishing a distinct maximum in $\chi(q)$. It is of course possible to obtain a maximum in $\chi(q)$ without the webbing feature in the Fermi surface, as long as we have sufficient area of Fermi surface separated by roughly the same wave vector Q. However, a detailed examination confirms their conclusion that the webbing is the only feature of the set of calculated Fermi surfaces that nests with roughly the right Q and shows the proper trend through the series, i.e., as one goes up the series of heavy rare earths, the webbing gets thicker and the helical structure gets more stable. This trend is further supported by the recent Fermi-surface calculation of Jackson for Tb.[10]

TABLE II. Magnetic ordering wave vectors (in units of π/c) as determined from experiment[a] and from the maximum in the theoretical susceptibilities.

Metal	Q_{expt}	Q_{theory} (with calculated E_F)	Q_{theory} (with E_F increased by 0.005 Ry from calculated E_F)
Dy1	0.49	0.60	0.53
Dy2		0.60	0.53
Er1	0.57	0.61	0.56
Er2		0.61	0.54
Lu	0.53	0.54	0.50

[a] Reference 6.

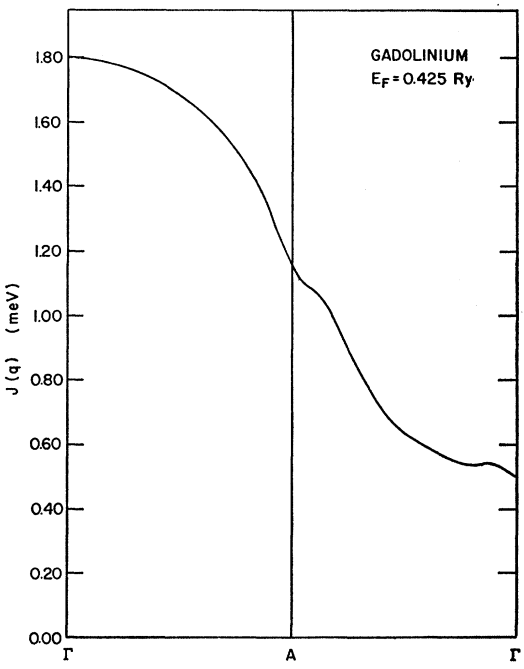

FIG. 5. $J(q)=I^2(q)\chi(q)$ for Gd.

We have pointed out above that the matrix elements associated with the generalized susceptibility should be decreasing functions of q. We have tried matrix elements of the form

$$I^2(q)=I^2(0)[e^{-\alpha q^2}+e^{-\alpha(4\pi/c-q)^2}]. \qquad (1.2)$$

We have chosen $I(0)=0.04$ eV and $\alpha=0.05c^2$ in order to make the width of $I(q)$ approximately correspond to the size of the $4f$ shell, and to normalize $J(q)=I^2(q)\chi(q)$ to approximately the size of $J(q)$ for Tb–10% Ho.[11] The second term in Eq. (1.2) makes $I^2(q)$ horizontal at the Brillouin-zone boundary. The result of applying $I^2(q)$ to our calculated susceptibilities is shown in Figs. 5 and 6. (The results for Er and Lu are very similar to those for Dy.) The $J(q)$ derived from the magnon spectra of Møller *et al.* is reproduced in Fig. 7. The similarity between the calculated and the experimental curves is rather striking. It is, however, apparent that

[10] C. Jackson, (to be published).

[11] H. Bjerrum Møller, J. C. G. Houmann, and A. R. Mackintosh, Phys. Rev. Letters **19**, 312 (1967).

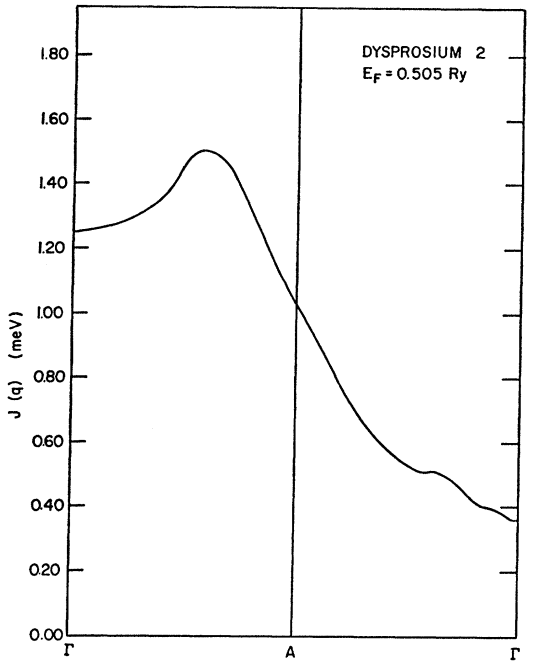

FIG. 6. $J(q)=I^2(q)\chi(q)$ for Dy.

the present work is still too crude to expect any meaningful quantitative comparison. The matrix element in Eq. (1.2) also shifts the maximum of $J(q)$ to a smaller q than that of $\chi(q)$.

Along with the similarity observed between the magnon spectrum of Tb–10% Ho and $\chi(q)$, we should also point out that bumps in the phonon spectrum of Y have been observed[12] which fit in nicely with the features we see in our calculated χ's. This is to be expected because the Fermi surface of Y[13] is very similar to that of the heavy rare earths, and the phonon spectrum should show Kohn anomalies at those

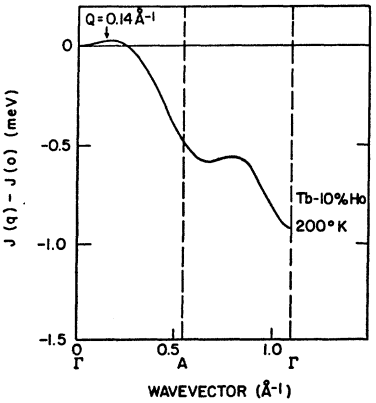

FIG. 7. $J(q)-J(0)$ for Tb–10% Ho from Ref. 10.

[12] T. O. Brun, S. K. Sinha, L. D. Muhlestein, and J. Sakurai, Bull. Am. Phys. Soc. 13, 450 (1968), and (to be published).
[13] T. L. Loucks, Phys. Rev. 144, 504 (1966).

q values corresponding to nesting Fermi surfaces. The magnon spectrum of Er measured by Woods *et al.*[14] does not show sufficient detail to compare with the important features of $\chi(q)$.

We can get some idea of how reasonable the magnitude of $\chi(Q)$-$\chi(0)$ is by a simple molecular field calculation. The Néel temperature T_N and the paramagnetic Curie temperature θ_P are related by

$$k(T_N-\theta_P)\cong\tfrac{1}{3}[I^2S(S+1)][\chi(Q)-\chi(0)]. \quad (1.3)$$

We find $[\chi(Q)-\chi(0)]\cong 6$ Ry^{-1} for Dy and 4.5 Ry^{-1} for Er. Taking $T_N=178.5$°K, $\theta_P=153$°K for Dy and $T_N=85$°K, $\theta_P=42$°K for Er, we find $I\sim 0.04$ to 0.09 eV. This value of $I(0)$ is consistent with other estimates.[15]

D. Variation of Q with Temperature

Neutron diffraction experiments revealed that the wave vectors of the periodic moment structure in heavy rare earths decrease as the temperature is reduced from the initial ordering temperature.[16] Three mechanisms have been recognized as the possible causes of this phenomenon: (1) The band splitting due to the ordering of the $4f$ moments[17,18]; (2) The magnetoelastic effect; and (3) The sixfold anisotropy in the basal plane.[19] We give here a brief derivation of the first effect based on a slightly different model than those used in Refs. 17 and 18. The magnetoelastic effect will be discussed in the next section. The anisotropy effect is not important in Tb and Dy because the sixfold anisotropy is negligibly small in the temperature range where the helical structure is stable.

If we postulate a one-dimensional parabolic band model

$$E_k=\hbar^2k^2/2m, \quad (1.4)$$

it is clear that $\chi(q)$ diverges logarithmically at $q=2k_F$. When the $4f$ moments are ordered in a helical state with wave vector q, the energy bands at k for one spin and at $k+q$ for the opposite spin are mixed according to

$$E_\pm=\tfrac{1}{2}\{E(k)+E(k+q) \pm([E(k)-E(k+q)]^2+V^2)^{1/2}\}, \quad (1.5)$$

where

$$V=I\sigma, \quad (1.6)$$

I is the s-f interaction matrix element (assumed to be a constant), and σ is the magnetic moment per spin.

[14] A. D. B. Woods, T. M. Holden, and B. M. Powell, Phys. Rev. Letters 19, 908 (1967).
[15] R. J. Elliott, in *Magnetism*, edited by G. T. Rado and H. Suhl (Academic Press Inc., New York, 1966), Vol. IIA, pp. 385–424; J. O. Dimmock and A. J. Freeman, Phys. Rev. Letters 13, 750 (1964).
[16] W. C. Kohler, E. O. Wollan, H. R. Child, and J. W. Cable, *Proceedings of the Third Conference on Rare-Earth Research, 1963* (Science Press, New York, 1964), p. 199.
[17] R. J. Elliott and F. A. Wedgwood, Proc. Phys. Soc. (London) 84, 63 (1964).
[18] Reference 3, Sec. IV.
[19] R. J. Elliott, Phys. Rev. 124, 346 (1961).

The new Fermi wave vectors are found from

$$E_+(k_{F+})=E_-(k_{F-}), \quad (1.7)$$

and the conservation of the number of particles. The energy of the system is

$$\mathcal{E}(q,V)=\int[E_+(k)f(E_+)+E_-(k)f(E_-)]dk, \quad (1.8)$$

where $f(E)$ is the Fermi distribution function. The result of this calculation is depicted in Fig. 8 for various values of q and V. In contrast to $\chi(q)$ the function $\mathcal{E}(q,V)$ does not diverge but has a minimum near $2k_F$ for small values of V. The position of the minimum determines the stable magnetic configuration. Since V increases with decreasing temperature according to Eq. (1.6), it is seen from Fig. 8 that the Q for the stable magnetic structure shifts to lower values. If V is large enough the ferromagnetic structure eventually becomes stable. The qualitative conclusions here are in complete agreement with the previous work, so we feel that they must be valid for general energy bands.

The fact that the ferromagnetic state may become stable for large V does not explain the ferromagnetic ground state of Tb and Dy, because in the theory Q vanishes continuously whereas the observed Q drops abruptly to zero from a finite value. It will be shown that this sudden change in magnetic structure can be explained by considering the magneto-elastic effect.

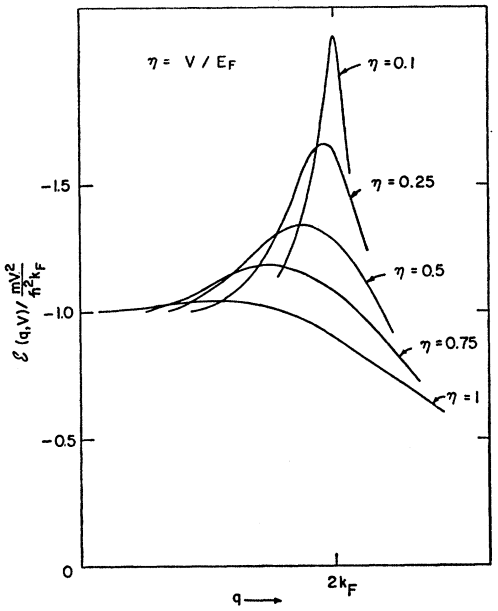

FIG. 8. Magnetic energy as function of q for several interaction strengths.

II. MAGNETO-ELASTIC EFFECT

A. Introduction

The magneto-elastic effect has been suggested by many authors as the driving force which stabilizes the ferromagnetic state in Tb and Dy at low temperatures.[20–23] The reasoning is as follows: The crystal lattice is coupled elastically to the magnetic system such that when the moments are aligned in a certain direction, the lattice becomes distorted somewhat in order to minimize the total energy. In the antiferromagnetic state, the magnetic moments cancel internally and so the lattice does not respond to the magnetic ordering. Cooper[23] called this the lattice clamping effect. It is easy to see that the antiferromagnetic state has a higher magneto-elastic energy than the ferromagnetic state. One can also show that the difference in elastic energy between the two states depends at least on the fourth power of the magnetization, so it is very small near the initial ordering temperature and much larger at lower temperatures. When added to the exchange energy, which favors periodic moment arrangement, the total energy of the crystal may favor a ferromagnetic state at sufficiently low temperatures.

Recently the magnetostriction and the anomalous thermal expansion of some rare earths have been measured on single crystals.[24–26] Meanwhile the basic theoretical formulation was worked out by Callen and Callen.[27,28] These developments enable us to make a detailed study of the connection between the magneto-elastic effect and the magnetic order transition. In order to adopt the Callen and Callen formalism to the helical spin structure, we have generalized it to allow nonuniform strain in the crystal. We will show that when the magnetic ordering is periodic, there is a thin layer at the surface of the crystal where the lattice is distorted with the same periodicity. The bulk of the material remains uniformly strained. The lattice is completely clamped with respect to certain components of the strain but only partially clamped for the other components. A study of the dependence of the elastic energy on the magnetic periodicity shows that the magneto-elastic effect also contributes to the temperature dependence of the magnetic Q in the helical region.

[20] C. Kittel, Phys. Rev. **120**, 335 (1960).
[21] U. Enz, Physica **26**, 698 (1960).
[22] E. W. Lee, Proc. Phys. Soc. (London) **84**, 693 (1964); Phys. Letters **4**, 358 (1963); R. G. Jordan and E. W. Lee, *ibid.* **92**, 1074 (1967).
[23] B. R. Cooper, Phys. Rev. Letters **19**, 900 (1967).
[24] S. Legvold, J. Alstad, and J. Rhyne, Phys. Rev. Letters **10**, 509 (1963).
[25] A. E. Clark, R. M. Bozorth, and B. F. DeSavage, Phys. Letters **5**, 100 (1963).
[26] A. E. Clark, B. F. DeSavage, and R. Bozorth, Phys. Rev. **138**, A216 (1965).
[27] E. R. Callen and H. B. Callen, Phys. Rev. **129**, 578 (1963).
[28] E. Callen and H. B. Callen, Phys. Rev. **139**, A455 (1965).

B. Formulation

The Hamiltonian for the crystal is written in the following form

$$H=H_m+H_e+H_1+H_2, \tag{2.1}$$

where H_m is the indirect exchange coupling term plus the part of anisotropy term which is not due to the strain. H_e is the elastic energy term, H_1 the one-ion contribution to the magneto-elastic energy, and H_2 the two-ion contribution. Presumably H_1 arises from crystalline field effects and H_2 from the spatial dependence of the indirect exchange. The elastic energy can be written down according to the standard method of lattice dynamics.[29] In particular, under uniform strain H_e is, as given in Ref. 28

$$H_e=\sum_{\Gamma}\sum_{j,j'}\tfrac{1}{2}c_{jj'}{}^{\Gamma}\sum_{i}\epsilon_i{}^{\Gamma,j}\epsilon_i{}^{\Gamma,j'}, \tag{2.2}$$

where the quantities c and ϵ are the elastic constants and the strain components respectively. The indices Γ, j, j' label the irreducible representations of the crystal group, and i labels the basis functions of the representation. The magneto-elastic energy terms are

$$\begin{aligned}H_1&=-\sum_f\sum_{\Gamma}\sum_{j,j'}\mathfrak{G}_{jj'}{}^{\Gamma}\sum_i \mathcal{E}_i{}^{\Gamma,j}(f)\mathcal{S}_i{}^{\Gamma,j'}(f),\\ H_2&=-\sum_{(f,g)}\sum_{\Gamma}\sum_{j,j'}\mathfrak{D}_{jj'}{}^{\Gamma}(f,g)\sum_i \mathcal{E}_i{}^{\Gamma,j}(f,g)\mathcal{S}_i{}^{\Gamma,j'}(f,g),\end{aligned} \tag{2.3}$$

where the functions $\mathcal{S}(f)$ and $\mathcal{S}(f,g)$ are the one-spin and two-spin basis functions tabulated in Ref. 27. The lattice sites are labeled by f and g, and the coupling constants by $\mathfrak{G}$ and $\mathfrak{D}(f,g)$. The functions $\mathcal{E}(f)$ and $\mathcal{E}(f,g)$ are the basis functions of the local strain constructed in the following manner: Let $\mathbf{R}_f{}^{(0)}=(X_f{}^{(0)},Y_f{}^{(0)},Z_f{}^{(0)})$ be the unstrained position vector of the lattice point f, and $\mathbf{r}_f=(x_f,y_f,z_f)$ be its displacement from the unstrained position, we can construct the following functions which are isomorphic to the strain tensors

$$\mathcal{E}_{xx}(f,g)=(X_f{}^{(0)}-X_g{}^{(0)})(x_f-x_g),$$

and similar expressions for $\mathcal{E}_{yy}$ and $\mathcal{E}_{zz}$, and

$$\begin{aligned}\mathcal{E}_{xy}(f,g)=\tfrac{1}{2}[&(X_f{}^{(0)}-X_g{}^{(0)})(y_f-y_g)\\&+(Y_f{}^{(0)}-Y_g{}^{(0)})(x_f-x_g)],\end{aligned} \tag{2.4}$$

and similar expressions for $\mathcal{E}_{yz}$ and $\mathcal{E}_{zx}$. Then the basis functions $\mathcal{E}_i{}^{\Gamma,j}(f,g)$ may be constructed out of these functions according to Table II of Ref. 28. The one-ion strain terms are obtained from $\mathcal{E}(f,g)$ by contraction

$$\mathcal{E}(f)=\sum_{\delta}\mathcal{E}(f,f+\delta), \tag{2.5}$$

where δ denotes the nearest neighbors of f.

The present formalism reduces to that in Ref. 28 in the ferromagnetic state. To show this we consider a simple cubic crystal with lattice parameter a. The free energy of the system is

$$F=E_m+E_e+\langle H_1\rangle+\langle H_2\rangle.$$

Since the strain is uniform we can express all components of $\mathcal{E}$ in terms of the strain tensor ϵ. For instance,

$$\mathcal{E}_{xx}(f,f+\delta)=a^2\epsilon_{xx}$$

if $\mathbf{R}_\delta{}^{(0)}$ is in the x direction, and

$$\mathcal{E}_{xx}(f,f+\delta)=0$$

otherwise. Also

$$\mathcal{E}_{xy}(f,f+\delta)=\tfrac{1}{2}a^2\epsilon_{xy}$$

if $\mathbf{R}_\delta{}^{(0)}$ is in either the x or y direction, and

$$\mathcal{E}_{xy}(f,f+\delta)=0$$

otherwise. In H_2 the expectation values of the spin functions $\langle\mathcal{S}(f,f+\delta)\rangle$ are the same for all nearest neighbors. Hence, when summed over all nearest neighbors, we obtain

$$\sum_{\delta}\mathcal{E}_i{}^{\Gamma j}(f,f+\delta)=2a^2\epsilon_i{}^{\Gamma j}.$$

We can then identify

$$\begin{aligned}2a^2\mathfrak{G}_{jj'}{}^{\Gamma}&=\tilde{B}_{jj'}{}^{\Gamma},\\ 2a^2\sum_{\delta}\mathfrak{D}_{jj'}{}^{\Gamma}(f,f+\delta)&=\sum_{\delta}\tilde{D}_{jj'}{}^{\Gamma}(f,f+\delta),\end{aligned}$$

where $\tilde{B}$, $\tilde{D}$ are the coupling constants defined in Ref. 28. For next nearest neighbors, we find the following relation between the coupling constants in the two theories

$$8a^2\sum_{g}\mathfrak{D}_{jj'}{}^{\Gamma}(f,g)=\sum_{g}\tilde{D}_{jj'}{}^{\Gamma}(f,g).$$

Similar relations may be found for more distant neighbor coupling constants. In an ideal hexagonal closed-packed crystal, where every ion has the same exchange interaction with all of its twelve nearest neighbors, one can show that

$$\begin{aligned}4a^2\mathfrak{G}_{jj'}{}^{\Gamma}&=\tilde{B}_{jj'}{}^{\Gamma}\\ 4a^2\sum_{\delta}\mathfrak{D}_{jj'}{}^{\Gamma}(f,f+\delta)&=\sum_{\delta}\tilde{D}_{jj'}{}^{\Gamma}(f,f+\delta),\end{aligned} \tag{2.6}$$

where a is the lattice parameter in the basal plane. For simplicity we limit ourselves to a nearest-neighbor model in the present discussion and will denote the two-ion magneto-elastic coupling constants simply by $\mathfrak{D}_{jj'}{}^{\Gamma}$.

C. Lattice Distortion in the Helical State

We demonstrate with a very simple model the effect of helical spin ordering on the lattice distortion. Consider a simple cubic crystal with nearest-neighbor elastic coupling. We label the lattice sites by integers

[29] See for example J. M. Ziman, *Electrons and Phonons* (Clarendon Press, Oxford, 1962), Chap. 1.

(l,m,n); then the elastic energy is

$$E_e=\tfrac{1}{2}\sum_{lmn}[K_1(x_{l+1,mn}-x_{lmn})^2+K_2(x_{l,m+1,n}-x_{lmn})^2 +K_2(x_{l,m,n+1}-x_{lmn})^2+\text{similar terms for } y \text{ and } z \text{ components}], \quad (2.7)$$

where K_1, K_2 are the spring constants. The specimen is assumed to be rectangular in shape with L, M, N unit cells on the edges. We consider only the $(\epsilon,2)$ component in the one-ion part of the magneto-elastic term. The general result becomes obvious after this disussion.

Consider a helical spin structure such that every xy plane is ferromagnetically ordered and the net moments of adjacent planes make an angle ψ. The spin functions involved in the term H_1 may be found to be

$$\langle \mathcal{S}_{1,2}^{\epsilon,2}(f)\rangle=0,$$
$$\langle \mathcal{S}_3^{\epsilon,2}(f)\rangle=\left(\frac{15}{16\pi}\right)^{1/2}\sin 2n\psi\,\mathfrak{L}(T),$$

where n is the z coordinate of the site f. The function $\mathfrak{L}(T)$ is the abbreviated notation of $\mathfrak{L}(T,0)$ of Ref. 28. At low temperatures $\mathfrak{L}(T)$ is proportional to the third power of the magnetization. Substituting into Eq. (2.3), we find the magneto-elastic coupling energy to be

$$\langle H_1\rangle=-\frac{15a}{16\pi}\mathfrak{K}^{\epsilon,2}\mathfrak{L}(T)\sum_{lmn}\sin 2n\psi \times\sum_{\delta}[(x_{l,m+\delta,n}-x_{lmn})+(y_{l+\delta,mn}-y_{lmn})], \quad (2.8)$$

where $\delta=\pm 1$. Most of the terms in the sum cancel out except those involving the displacement of the surface atoms. The above expression reduces to

$$\langle H_1\rangle=-B(T)\sum_{lmn}\sin 2n\psi\,[(x_{lMn}-x_{l0n})-(y_{Lmn}-y_{0mn})], \quad (2.9)$$

where we group together a number of factors and call them $B(T)$. To find the equilibrium lattice distortion we minimize $E_e+\langle H_1\rangle$ with respect to the displacements. For the x components the equilibrium conditions are

$$K_1(2x_{lmn}-x_{l+1,mn}-x_{l-1,mn}) +K_2(2x_{lmn}-x_{l,m+1,n}-x_{l,m-1,n}) +K_2(2x_{lmn}-x_{lm,n+1}-x_{lm,n-1})=0 \quad (2.10)$$

for a point (l,m,n) inside the crystal. On the surfaces $m=0$ and M, we find

$$K_1(2x_{l0n}-x_{l+1,0n}-x_{l-1,0n})+K_2(x_{l0n}-x_{l1n}) +K_2(2x_{l0n}-x_{l0,n+1}-x_{l0,n-1})=-F,$$
$$K_1(2x_{lMn}-x_{l+1,Mn}-x_{l-1,Mn})+K_2(x_{lMn}-x_{l,M-1,n}) +K_2(2x_{lMn}-x_{lM,n+1}-x_{lM,n-1})=F, \quad (2.11)$$

where

$$F=B(T)\sin 2n\psi.$$

Try a solution of the form

$$x_{lmn}=\int A(\xi,\eta,\zeta)e^{i(\xi l+\eta m+\zeta n)}d\xi d\eta d\zeta,$$

then from Eq. (2.10) one finds

$$K_1(1-\cos\xi)+K_2(1-\cos\eta)+K_2(1-\cos\zeta)=0. \quad (2.12)$$

From Eq. (2.11) we obtain

$$\int A(\xi,\eta,\zeta)[K_1(1-\cos\xi)+K_2(1-e^{in})+K_2(1-\cos\xi)] \times e^{i(\xi l+\zeta n)}d\xi d\eta d\zeta=-F. \quad (2.13)$$

Combining Eqs. (2.12) and (2.13), we find

$$i\int A(\xi,\eta,\zeta)K_2\sin\eta e^{i(\xi l+\zeta n)}d\xi d\eta d\zeta=-B(T)\sin 2n\psi.$$

By comparing the l, n dependence on both sides, one obtains

$$\xi=0,$$
$$\zeta=\pm 2\psi.$$

Substituting into Eq. (2.12), one obtains the following relation between η and ψ:

$$\cos\eta=2-\cos 2\psi>0.$$

Thus η is purely imaginary and the solution for x_{lmn} is damped out as one moves away from the surface. The interlayer turn angle in rare earths is around 50°. This gives

$$\cos\eta\cong 2$$

or

$$|\eta|\cong 1.3.$$

The thickness of the surface layer is only a few lattice parameters. The bulk of the crystal remains unstrained. This is a microscopic demonstration of the lattice clamping effect. Although the theory is based on a very simple model, the result should have general validity.

The elastic energy associated with the lattice distortion is proportional to the surface area, and is therefore negligible compared with other volume effects.

D. Application to Dy

We apply our theory of the magneto-elastic effect to Dy because it has been extensively investigated experimentally.[26] Dy has a hexagonal closed-packed structure. It is ferromagnetic below 85°K and has a helical structure between 85 and 179°K.[16] The magnetic ordering transition at 85°K is of the first order and is accompanied by a spontaneous change in lattice pa-

rameters.[30] The magnetic properties of Dy are highly anisotropic such that the moments are confined in the basal plane in the ordered state. Below 90°K the a axis in the hexagonal plane is the easy direction.[31] We choose a coordinate system where the a, b, and c axes are the x, y, and z directions, respectively.

From magnetostriction studies Clark *et al.*[26] concluded that magneto-elastic effects in Dy can be described to a high degree of accuracy by keeping only the $(\gamma,2)$ and $(\epsilon,2)$ terms in H_1 and $(\alpha,1)$ and $(\alpha,2)$ terms in H_2.[32] We use the same notation for the irreducible representations as in Ref. 27. Since the moments are restricted in the basal plane, the $(\epsilon,2)$ terms do not enter the theory as long as there is no external field. The elastic constants of Dy have been measured on a single crystal at room temperature and above by Fisher and Dever.[33] Their data show that

$$c_{12}{}^{\alpha}=0,$$

so that the $(\alpha,1)$ and $(\alpha,2)$ representations of the stress tensor are not coupled. Hence, the relevant elastic and magneto-elastic energies are given by the following expressions:

$$\begin{aligned}
&E_e=\tfrac{1}{2}c_{11}{}^{\alpha}(\epsilon^{\alpha,1})^2+\tfrac{1}{2}c_{22}{}^{\alpha}(\epsilon^{\alpha,2})^2+\tfrac{1}{2}c^{\gamma}(\epsilon^{\gamma})^2,\\
&\langle H_1\rangle=-\sum_f \mathcal{B}^{\gamma}[\mathcal{E}_1{}^{\gamma}(f)\langle \mathcal{S}_1{}^{\Gamma,2}(f)\rangle\\
&\qquad\qquad +\mathcal{E}_2{}^{\gamma}(f)\langle \mathcal{S}_2{}^{\Gamma,2}(f)\rangle], \qquad (2.14)\\
&\langle H_2\rangle=-\sum_{f,\delta}\sum_{j,j'} \mathfrak{D}_{jj'}{}^{\alpha}\mathcal{E}^{\alpha,j}(f,f+\delta)\langle \mathcal{S}^{\alpha j'}(f,f+\delta)\rangle.
\end{aligned}$$

We now evaluate the expectation values of the spin functions. In the ferromagnetic state with moments aligned in the x direction

$$\begin{aligned}
&\langle \mathcal{S}^{\alpha,1}(f,f+\delta)\rangle=\mathcal{J}_{\delta}(T),\\
&\langle \mathcal{S}^{\alpha,2}(f,f+\delta)\rangle=-(1/2\sqrt{3})\mathcal{L}_{\delta}(T),\\
&\langle \mathcal{S}_1{}^{\gamma}(f)\rangle=\tfrac{1}{2}\mathcal{L}(T),\\
&\langle \mathcal{S}_2{}^{\gamma}(f)\rangle=0,
\end{aligned} \qquad (2.15)$$

where $\mathcal{J}_{\delta}(T)$, $\mathcal{L}_{\delta}(T)$, $\mathcal{L}(T)$ are the abbreviated notations for $\mathcal{J}_{f,f+\delta}(T,0)$, $\mathcal{L}_{f,f+\delta}(T,0)$ and $\mathcal{L}_f(T,0)$ in Ref. 28. Since the strain is uniform we may use the relation in Eq. (2.6) to reduce $\langle H_1\rangle$ and $\langle H_2\rangle$ to

$$\begin{aligned}
&\langle H_1\rangle=-\tfrac{1}{2}N\tilde{B}^{\gamma}\epsilon^{\gamma}\mathcal{L}(T),\\
&\langle H_2\rangle=-\tfrac{1}{2}N\sum_{\delta}\Big[\tilde{D}_{11}{}^{\alpha}\epsilon^{\alpha,1}\mathcal{J}_{\delta}(T)-\frac{1}{2\sqrt{3}}\tilde{D}_{12}{}^{\alpha}\epsilon^{\alpha,1}\mathcal{L}_{\delta}(T)\\
&\qquad +\tilde{D}_{21}{}^{\alpha}\epsilon^{\alpha,2}\mathcal{J}_{\delta}(T)-\frac{1}{2\sqrt{3}}\tilde{D}_{22}{}^{\alpha}\epsilon^{\alpha,2}\mathcal{L}_{\delta}(T)\Big]. \qquad (2.16)
\end{aligned}$$

N is the total number of atoms in the crystal. Minimizing the total energy with respect to the strain tensors, we find the equilibrium strains to be

$$\begin{aligned}
&\epsilon^{\alpha,1}=\lambda_1, \quad \epsilon^{\alpha,2}=\lambda_2,\\
&\epsilon_1{}^{\gamma}=\tfrac{1}{2}\lambda^{\gamma}, \quad \epsilon_2{}^{\gamma}=0,
\end{aligned}$$

where

$$\begin{aligned}
&\lambda_1=\frac{N}{2c_{11}{}^{\alpha}}\sum_{\delta}\Big[\tilde{D}_{11}{}^{\alpha}\mathcal{J}_{\delta}(T)-\frac{1}{2\sqrt{3}}\tilde{D}_{12}{}^{\alpha}\mathcal{L}_{\delta}(T)\Big],\\
&\lambda_2=\frac{N}{2c_{22}{}^{\alpha}}\sum_{\delta}\Big[\tilde{D}_{21}{}^{\alpha}\mathcal{J}_{\delta}(T)-\frac{1}{2\sqrt{3}}\tilde{D}_{22}{}^{\alpha}\mathcal{L}_{\delta}(T)\Big], \qquad (2.17)\\
&\lambda^{\gamma}=\frac{N}{c^{\gamma}}\tilde{B}^{\gamma}\mathcal{L}(T).
\end{aligned}$$

The total elastic energy at equilibrium is then

$$\begin{aligned}
&E_e+\langle H_1\rangle+\langle H_2\rangle\\
&\qquad =-\tfrac{1}{2}c_{11}{}^{\alpha}(\lambda_1)^2-\tfrac{1}{2}c_{22}{}^{\alpha}(\lambda_2)^2-\tfrac{1}{8}c^{\gamma}(\lambda^{\gamma})^2. \qquad (2.18)
\end{aligned}$$

In the helical state,

$$\begin{aligned}
&\langle \mathcal{S}^{\alpha,1}(f,f+\delta)\rangle=\mathcal{J}_{\delta}(T),\\
&\langle \mathcal{S}^{\alpha,2}(f,f+\delta)\rangle=-(1/2\sqrt{3})\mathcal{L}_{\delta}(T),
\end{aligned}$$

if $f+\delta$ is one the same basal plane as f, and

$$\begin{aligned}
&\langle \mathcal{S}^{\alpha,1}(f,f+\delta)\rangle=\mathcal{J}_{\delta}(T)\cos\psi,\\
&\langle \mathcal{S}^{\alpha,2}(f,f+\delta)\rangle=-(1/2\sqrt{3})\mathcal{L}_{\delta}(T)\cos\psi,
\end{aligned} \qquad (2.19)$$

if $f+\delta$ is on a different basal plane, $\psi=$ interlayer turn angle. The quantities

$$\begin{aligned}
&\langle \mathcal{S}_1{}^{\gamma}(f)\rangle=\tfrac{1}{2}\mathcal{L}(T)\cos 2n\psi,\\
&\langle \mathcal{S}_2{}^{\gamma}(f)\rangle=\tfrac{1}{2}\mathcal{L}(T)\sin 2n\psi,
\end{aligned}$$

where n labels the basal plane of the site f. From the previous discussion we conclude that the $(\gamma,2)$ component of the strain is completely clamped. The $(\alpha,1)$ and $(\alpha,2)$ components of the local strain are

$$\begin{aligned}
&\sum_{\delta}\mathcal{E}^{\alpha,1}(f,f+\delta)=2a^2(\epsilon^{\alpha,1}-\sqrt{3}\epsilon^{\alpha,2}),\\
&\sum_{\delta}\mathcal{E}^{\alpha,2}(f,f+\delta)=-(1/\sqrt{3})a^2(\epsilon^{\alpha,1}-\sqrt{3}\epsilon^{\alpha,2}),
\end{aligned}$$

where $f+\delta$ is on the same basal plane as f, and

$$\begin{aligned}
&\sum_{\delta}\mathcal{E}^{\alpha,1}(f,f+\delta)=2a^2(\epsilon^{\alpha,1}+\sqrt{3}\epsilon^{\alpha,2}),\\
&\sum_{\delta}\mathcal{E}^{\alpha,2}(f,f+\delta)=a^2[(1/\sqrt{3})\epsilon^{\alpha,1}+3\epsilon^{\alpha,2}],
\end{aligned}$$

where $f+\delta$ is on a different basal plane. Hence

$$\begin{aligned}
&\langle H_1\rangle=0,\\
&\langle H_2\rangle=-[\tfrac{1}{2}c_{11}{}^{\alpha}\lambda_1(1+\cos\psi)\\
&\qquad -(1/4\sqrt{3})c_{22}{}^{\alpha}\lambda_2(1-\cos\psi)]\epsilon^{\alpha,1}\\
&\qquad +[-\tfrac{1}{2}\sqrt{3}c_{11}{}^{\alpha}\lambda_1(1-\cos\psi)\\
&\qquad\qquad +\tfrac{1}{4}c_{22}{}^{\alpha}\lambda_2(1+3\cos\psi)]\epsilon^{\alpha,2},
\end{aligned} \qquad (2.20)$$

[30] F. J. Darnell and E. P. Moore, J. Appl. Phys. **34**, 1337 (1963). V. A. Finkel and V. V. Vorobev, Zh. Eksperim. i Teor. Fiz. **51**, 786 (1966) [English transl.: Soviet Phys.—JETP **24**, 524 (1967)].

[31] D. R. Behrendt, S. Legvold, and F. H. Spedding, Phys. Rev. **109**, 1544 (1958).

[32] See also the review article by E. Callen, J. Appl. Phys. **39**, 519 (1968).

[33] E. S. Fisher and D. Dever, Trans. Met. Soc. AIME **239**, 48 (1967).

where λ_1, λ_2 are defined in Eq. (2.17). Again the equilibrium strains are found by minimizing the total energy:

$$\epsilon^{\alpha,1}=\tfrac{1}{2}\lambda_1(1+\cos\psi)-(1/4\sqrt{3})(c_{22}{}^{\alpha}/c_{11}{}^{\alpha})\lambda_2(1-\cos\psi),$$
$$\epsilon^{\alpha,2}=\tfrac{1}{4}\lambda_2(1+3\cos\psi)-\tfrac{1}{2}\sqrt{3}(c_{11}{}^{\alpha}/c_{22}{}^{\alpha})\lambda_1(1-\cos\psi), \quad (2.21)$$
$$\epsilon_1{}^{\gamma}=\epsilon_2{}^{\gamma}=0.$$

The $\epsilon^{\alpha,1}$, $\epsilon^{\alpha,2}$ components are partially clamped in the helical state. The total elastic energy is

$$E_e+\langle H_1\rangle+\langle H_2\rangle=-\tfrac{1}{2}c_{11}{}^{\alpha}(\epsilon^{\alpha,1})^2-\tfrac{1}{2}c_{22}{}^{\alpha}(\epsilon^{\alpha,2})^2. \quad (2.22)$$

We can relate the strain tensor to the anomalous thermal expansion along the symmetry axes by

$$(\delta l/l)_x=\tfrac{1}{3}\epsilon^{\alpha,1}-\tfrac{1}{3}\sqrt{3}\epsilon^{\alpha,2}+\epsilon_1{}^{\gamma},$$
$$(\delta l/l)_y=\tfrac{1}{3}\epsilon^{\alpha,1}-\tfrac{1}{3}\sqrt{3}\epsilon^{\alpha,2}-\epsilon_1{}^{\gamma}, \quad (2.23)$$
$$(\delta l/l)_z=\tfrac{1}{3}\epsilon^{\alpha,1}+\tfrac{2}{3}\sqrt{3}\epsilon^{\alpha,2}.$$

We see from these results that the anomalous thermal expansion must change abruptly at the transition temperature between the ferromagnetic and the helical states because ψ changes abruptly there. Furthermore, the anomalous thermal expansion along the a and b axes are the same in the helical spin state but become different in the ferromagnetic state. Using the data in Ref. 26 for the anomalous thermal expansion and the interlayer turn angle $\psi=27°$ just above 85°K, we find the quantities λ_1 and λ_2 to be

$$\lambda_1=-2.5\times10^{-3},$$
$$\lambda_2=3.24\times10^{-3}.$$

If we approximate both $\mathcal{J}_\delta(T)$ and $\mathcal{L}_\delta(\mathcal{L})$ by σ^2, where σ is the magnetization, we can calculate the anomalous thermal expansion at higher temperatures. The results are plotted in Figs. 9 and 10 along with the experimental curves. The agreement is reasonably good. The discrepancy is possibly due to our neglect of the higher-order representations of the magneto-elastic coupling terms.

At the ferro-helical transition point the elastic constants change abruptly, as found by Rosen.[34] The Young's modulus changes from 5.7×10^{11} dyn/cm² just below 85°K to 6.9×10^{11} dyn/cm² just above 85°K. The measurement was not done on a single crystal, but we may assume that the individual elastic constants vary in the same ratio as the average elastic moduli. If the magneto-elastic coupling remains constant at the transition, then, since λ_1 and λ_2 are inversely proportional to the elastic constants, their values in the ferromagnetic state should be

$$\lambda_1=-3.0\times10^{-3},$$
$$\lambda_2=3.9\times10^{-3}.$$

[34] M. Rosen, Phys. Rev. (to be published).

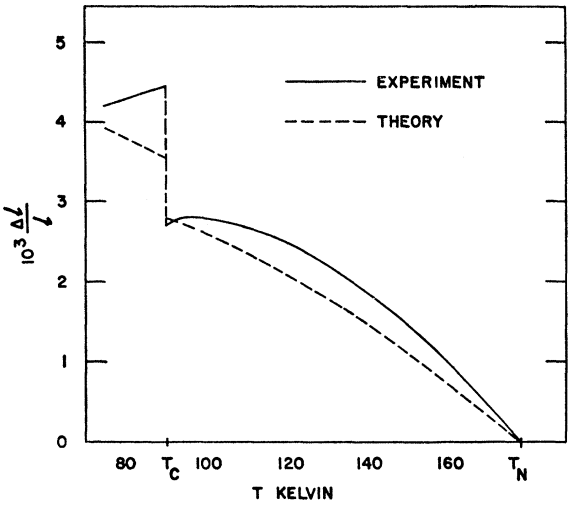

FIG. 9. The anomalous thermal expansion of Dy along the c axis of the crystal.

From these we compute the thermal expansion along the c axis and the average thermal expansion along the a and b axes. The results are also shown on Figs. 9 and 10. The disagreement between the theoretical and experimental values is relatively large. From the experimental strains in the ferromagnetic state, we find

$$\lambda_1=-3.0\times10^{-3},$$
$$\lambda_2=4.7\times10^{-3}.$$

The large discrepancy for λ_2 seems to indicate that some higher-order representations of the magneto-elastic coupling have been left out, or that our way of scaling the temperature dependence of the elastic constants is too naive.

Finally, we calculate the difference in elastic energy between the helical and the ferromagnetic states at

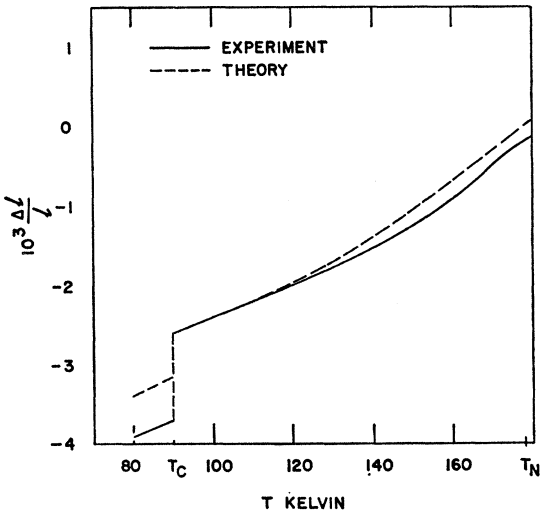

FIG. 10. The average anomalous thermal expansion of Dy along the a and b axes.

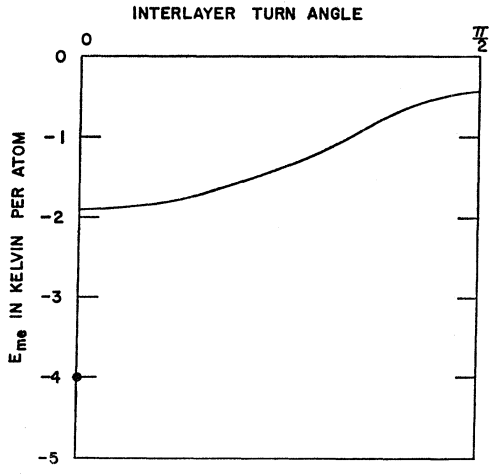

FIG. 11. The total magneto-elastic energy of Dy in the helical state as a function of the interlayer turn angle. The curve is computed using the energy parameters just above 85°K. The energy of the ferromagnetic state just below 85°K is represented by a dot at $\psi=0$, $E_{me}=-4.0$ K/atom.

85°K. We use as much as possible the experimentally measured quantities. One finds from the data of Fisher and Dever[33] that

$$c_{11}^{\alpha}=4.11\times10^{11},$$
$$c_{22}^{\alpha}=11.27\times10^{11},$$
$$c^{\gamma}=9.7\times10^{11}\ \text{dyn/cm}^2,$$

at room temperature. If we apply the temperature correction as found by Rosen, we estimate

$$c_{11}^{\alpha}=4.5\times10^{11},$$
$$c_{22}^{\alpha}=12.4\times10^{11}\ \text{dyn/cm}^2,$$

just above 85°K, and

$$c_{11}^{\alpha}=3.7\times10^{11},$$
$$c_{22}^{\alpha}=10.2\times10^{11},$$
$$c^{\gamma}=8.65\times10^{11}\ \text{dyn/cm}^2,$$

just below 85°K. Thus, the elastic energies are found to be

$$E_f=-1.66\ J/\text{cm}^3$$

for the ferromagnetic state, and

$$E_h=-0.72\ J/\text{cm}^3$$

for the helical state. The difference

$$\Delta E=0.94\ J/\text{cm}^3 \text{ or } 2.2\ \text{K/atom}$$

is equal to the difference between the exchange energies of these two states. The latter quantity was estimated by Jordan and Lee[22] to be 0.7 J/cm^3 and by Cooper[23] as 0.8 K/atom. Our value is in accord with both estimates. This shows that the magneto-elastic effect is the principal driving force which stabilizes the ferromagnetic state.

One can see from Eqs. (2.18) and (2.22) that the $(\alpha,1)$ and $(\alpha,2)$ components of the magneto-elastic energy depends on the temperature like σ^4 and the $(\gamma,2)$ component like σ^6. Hence, the magneto-elastic energy is relatively unimportant at the initial ordering temperature, but may compete with the exchange energy in the determination of the stable magnetic structure at lower temperatures.

In Fig. 11 we plot the variation of the elastic energy with the interlayer turn angle using the parameters just above 85°K. We can see that the elastic energy always favors smaller turn angle. This also helps to shift the magnetic Q to a lower value than that determined from the Fermi-surface geometry.

The conical ferromagnetic state in Er and Ho at low temperatures is stabilized by a combination of magneto-elastic and anisotropy effects. The elastic energies of the conical and modulated moment states in Ho, Er, and Tm may be calculated in a way analogous to the helical structure. The effect of anisotropy on the magnetic ordering has been discussed in detail by Kaplan[35] and Elliott[19] and there is no need for further elaboration.

[35] T. A. Kaplan, Phys. Rev. 124, 329 (1961).